

Optimization of RF Excitation to Maximize Signal and T2 Contrast of Tissues with Rapid Transverse Relaxation

M. Carl¹, M. Bydder², J. Du², A. Takahashi¹, E. Han¹, and G. Bydder²
¹GE Healthcare, Waukesha, WI, United States, ²University of California, San Diego

Introduction: Traditional MRI is predominantly geared towards the imaging of long T_2 species, for which the RF duration τ can be considered negligible compared to the intrinsic T_2 of the tissues imaged. When using UTE methods to image short or ultra short T_2 species, such as ligaments, tendons or cortical bone, the intrinsic T_2 can be on the same order as τ , and the signal decay during the RF pulse may no longer be ignored [1,2]. In prior work [3,4] we presented theoretical results on how to select the parameters of a non-selective SPGR RF pulse train to maximize signal amplitude and T_2 contrast for these circumstances. Here, we present experiments conducted to verify our theoretical findings.

Theory: In prior work, we derived a closed form analytic expression, called the generalized Ernst angle equation, for the optimum duration of a hard RF pulse train with amplitude of B_1 ($\omega_1 = \gamma B_1$) to maximize the MR signal in the presence of T_2 relaxation [3]:

$$\cos\left(\sqrt{\omega_1^2 - \frac{1}{4T_2^2}} \tau\right) - \frac{1}{2T_2 \sqrt{\omega_1^2 - \frac{1}{4T_2^2}}} \sin\left(\sqrt{\omega_1^2 - \frac{1}{4T_2^2}} \tau\right) = \exp\left(-\frac{TR}{T_1}\right) \exp\left(-\frac{\tau}{2T_2}\right) \quad (1)$$

To maximize T_2 contrast generated by the RF pulse itself, the optimum flip angle is simply the classical Ernst angle and the optimum pulse duration is directly proportional to the average T_2 of the tissues of interest. The proportionality factor $\kappa \equiv \tau/T_2$ for the optimum pulse duration depends on TR/T_1 and can be solved numerically [4] and is displayed in Fig. 1.

Experimental Design: In order to verify the theoretical results, phantom tests were performed on an array of six syringes filled with water doped with various concentrations of $MnCl_2$ (resulting in $T_2^* \approx T_2$) and arranged in a single plane. The imaging sequence used in these experiments consisted of non-selective hard pulse excitation, followed by a 2D radial UTE k-space acquisition ($TE = 12 \mu s$) within the plane of the array of syringes, resulting in a projection image through the slice direction.

The measured T_1 and T_2^* of the six syringes are summarized in columns two and three of Table I. Due to the rapid transverse relaxation during the RF pulse, T_1 quantification using saturation-recovery or inversion recovery sequences are impractical for the shorter T_2 phantoms. Therefore, T_1 measurements were performed using UTE imaging with a very short RF duration ($\tau = 24 \mu s$) and high RF amplitude ($B_1 = 23 \mu T$), resulting in a flip angle of approximately $\theta = \gamma B_1 \tau = 8.7^\circ$. With such short τ , the T_2 decay during the RF pulse was assumed negligible. The acquisitions were repeated at various values for TR and then fitted to the classical SPGR steady state signal equation. T_2^* measurements were performed using the same sequence but varying TE .

Signal Optimization: To validate the generalized Ernst angle equation, the set of six syringes were imaged multiple times – each with a different RF excitation pulse duration, but fixed RF amplitude. The TR was fixed at 100 ms. The MR signal intensities were measured within each phantom, and are plotted as a function of nominal flip angle (and hence pulse duration) in Fig. 2. In order to purposefully emphasize T_2 decay during the RF pulse, the results were obtained using a small value of $B_1 = 2 \mu T$ resulting in long RF durations of $\tau = 200 \mu s$ – $3000 \mu s$ to achieve the range of flip angles displayed. The experimental results displayed in Fig. 2 can be readily compared with our theoretical predictions. For this purpose, the two right columns of Table I show the expected values for the classical Ernst angle and generalized Ernst angle. For all curves in Fig. 2, one can see a good agreement between the predicted optimum flip angles (“Generalized Ernst” in Table I) using Eq. [1] and the locations of the experimentally measured signal intensity peaks. To further highlight this fact, the experimental procedure leading to Fig. 2 was repeated using different values for B_1 and TR . Fig. 3 shows a scatter plot of the experimentally measured optimum flip angles vs. the corresponding theoretical values. The six filled markers correspond to the data for Syringes 1 & 2, for which the generalized Ernst angle is significantly lower than the classical Ernst angle.

Contrast Optimization: The next experimental study was conducted to verify the optimum RF pulse duration τ , to maximize signal contrast between tissues of different T_2^* values. We focused on syringes 1 and 2, which have the shortest and also most closely matched values of T_2^* (as well as T_1). As before, UTE images were obtained using several different RF durations. The echo time parameter was chosen extremely short at $TE = 12 \mu s$ to ensure that the T_2 contrast is dominated by the RF pulse itself. The TR 's in these experiments were chosen to be $TR = 300 ms$ and $TR = 50 ms$, resulting in $TR/T_1 \approx 4$ and $TR/T_1 \approx 0.7$ respectively. Based on our theoretical results on optimizing the T_2 contrast [4], the flip angles were chosen to be the classical Ernst angle ($\theta \approx 90^\circ$ for $TR = 300 ms$ and $\theta \approx 60^\circ$ for $TR = 50 ms$). The signal difference (contrast) between the two phantoms is plotted as a function of τ in Fig. 4. As one can observe, the contrast for $TR = 300 ms$ is maximized at around $\tau \approx 800 \mu s$, while the contrast for $TR = 50 ms$ is maximized at around $\tau \approx 1000 \mu s$ in agreement with our theoretically predicted values from Fig. 1: For $TR = 300 ms \rightarrow \tau \approx 1.71 \cdot T_2 = 846 \mu s$ and for $TR = 50 ms \rightarrow \tau \approx 2.1 \cdot T_2 = 1040 \mu s$.

Conclusion: It was shown that the experimental data very closely matched the theory for both the signal (SNR) optimization as well as the contrast (CNR) optimization. Therefore, the simple guidelines on optimizing MR signal and T_2 contrast can directly be implemented to maximize the scan efficiency of UTE acquisitions, for which non-selective hard pulses are used.

References: [1] Tyler et al, JMRI 25:279 (2007) [2] Sussman et al, MRM 40:890 (1998) [3] Carl et al, ISMRM 2009, p.4343 [4] Carl et al, ISMRM 2009, p.4375

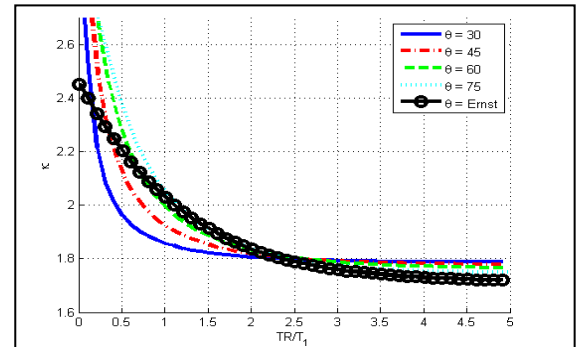


Fig. 1: Optimum $\kappa \equiv \tau/T_2$ for a SPGR sequence as a function of TR/T_1 .

| Syringe | T_1 [ms] | T_2^* [ms] | Ernst | Gen. Ernst |
|---------|------------|--------------|-------|------------|
| 1 | 73 | 0.43 | 75.28 | 38.56 |
| 2 | 85 | 0.56 | 72.04 | 42.00 |
| 3 | 97 | 2.73 | 69.10 | 60.39 |
| 4 | 160 | 6.9 | 57.64 | 54.96 |
| 5 | 345 | 18 | 41.55 | 41.02 |
| 6 | 2300 | 125 | 16.77 | 16.77 |

Table I: MR relaxation properties and classical as well as generalized Ernst angle for the data displayed in Fig. 2.

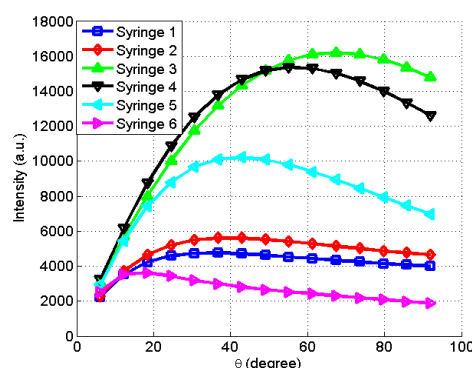


Fig. 2: Signal intensity as a function of excitation flip angle using a fixed RF amplitude of $B_1 = 2 \mu T$ and $TR = 100 ms$ for the six different phantoms in Table I.

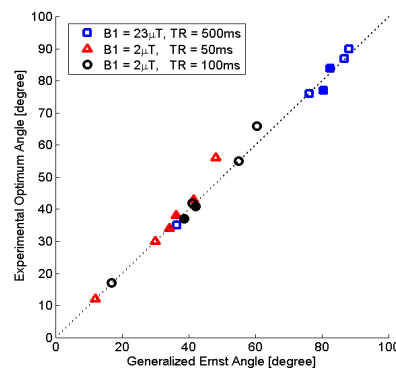


Fig. 3: Scatter plot of the experimentally measured optimum flip angles vs. the corresponding theoretical values. The filled markers correspond to the data for Syringes 1 & 2. Also shown is a dotted reference line of slope one.

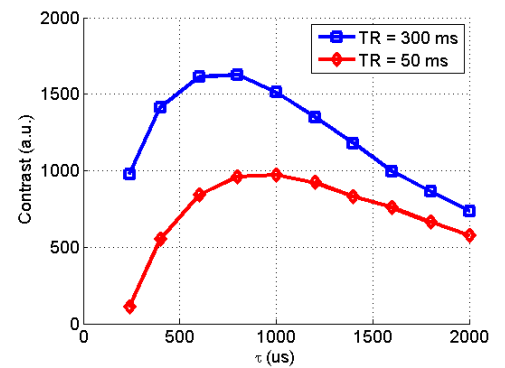


Fig. 4: Signal difference between syringes 1 and 2 of Table 1 as a function of the RF pulse duration τ using $TR = 300 ms$ with $\theta = 90^\circ$ (squares), and $TR = 50 ms$ with $\theta = 60^\circ$ (diamonds).